Achieving
Full Astrometric Accuracy with MICADO and Requirements for the MICADO ADC

Table of Contents

Executive Summary

The relative astrometric accuracy of MICADO is required to be better than 50 micro arcseconds relative over the FoV. This means that the contribution of the ADC must be less than 10 micro arcseconds, while the atmospheric dispersion over the observed band reaches 0.5 arcseconds (500000 micro arcseconds) and the absolute atmospheric refraction reaches 20 arcseconds (20000000 micro arcseconds). The performance of the MICADO ADC was not studied during the Phase A study.

In this study we investigate the important parameters for astrometry related to the ADC. Two different ADC designs have been investigated: an ADC in the pupil plane and an ADC close to the Image plane. Detailed simulations have been performed to quantify the astrometric effects including: Field dependency, wavelength dependency, Zenith Distance dependency, temperature dependency, total effect on various star types. It is demonstrated that a temperature stabilized pupil plane ADC is the preferred solution.

Different requirements have been identified for imaging, photometry and astrometry. A draft observational strategy is presented that includes:

- An inline ADC correction using atmospheric parameters to reach imaging requirements.
- An offline ADC distortion correction to reach photometry requirements while stacking images.
- An offline physical model correcting the distortion created by atmospheric parameters, ADC parameters and the spectral type of observed stars in order to reach astrometric requirements.

What can be concluded at this time is that the only way to achieve micro arcsecond astrometry is to do a real time correction of atmospheric effects using the ADC hardware, combined with post processing of the data using a physical model of the relevant parts and parameters of the instrument and atmosphere.
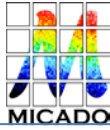
1   Introduction

This study was triggered by the requirements set on the astrometric accuracy, the subsequent requirements on the Atmospheric Dispersion Corrector (ADC) and to understand if and under which conditions The Netherlands could accept the ADC work package. The general feeling is that in order to develop an ADC that does not impact the astrometry, the requirements on this ADC would make this ADC not feasible. The subject was never investigated during the MICADO phase A study, because the ADC was first in the ESO Telescope work package and was moved to the instrumentation work packages shortly before the end of the phase A study. The current study aims at investigating:

- the requirements on the astrometric accuracy as defined by the phase A study
- the impact on the required accuracy of the ADC
- understanding the internal and external factors that impact the accuracy of atmospheric dispersion correction and developing a model for it
- the cross-talk between the operation of the ADC and other factors on the atmospheric precision
- potential for calibration
- to give a set of realistic requirements on the astrometric accuracy and ADC that can be achieved

2   Identification of issues and first order estimates

2.1   Current knowledge on AO and Astrometry

Keck (SCAO). With the Keck SCAO system, an accuracy of ~100 micro arcsecond has been achieved under good conditions, but the paper also states: "Some AO architectures (i.e. MCAO) could yield significantly worse plate scale stability due to unsensed modes between deformable mirrors, which lead to overall field (de)magnification. The timescales over which these modes operate are currently unknown, and will likely be a function of the system architecture and control loop design."

VLT MAD (MCAO). In her PhD thesis, Eva Meyer found with MAD (ESO's MCAO Demonstrator for the VLT) a positional precision for stars between K = 14 – 18 mag of ≈ 1.2 milli arcsecond in the full MCAO correction mode data of the cluster NGC 6388.

GEMS (MCAO). The Gemini MCAO team with experts like Francois Rigaut (who has been working on MCAO for more than 15 years) report in "GeMS, first on-sky results", Rigaut et al., SPIE, 2012: "Using averages of two images taken 3mn apart, the median separation error is of the order of 1.1 mas over the whole separation range. It is smaller for small separations, down to 600 micro-arcseconds for separation smaller than 5 arcseconds. Note that this is the error on the separation, so that providing enough references stars around the object of interest, this can be reduced by ~sqrt(2), leading to an astrometric error of 420 micro-arcseconds. From our reduced data set, there is no evidence that we reach any kind of systematics, so that further averaging will likely further reduce the astrometric error." Also note that this is still a factor of 10 worse than what MICADO requires. One problem is the time variability. They conclude that "the need
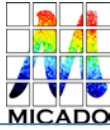
to control plate scale/rotation in addition to simple position, MCAO raises the complexity of the problem."

Palomar + PALOA/PHARO (SCAO). ~0.1 mas in 2 minutes, ~0.05 mas expected in 15 min, stable over months (Cameron 2009). In this case it needs to be noted that this is a relatively small telescope with a monolithic mirror, significantly improving the stability of the system.

2.2 The astrometric requirements for MICADO

According to the "MICADO Compliance Matrix" (E-TRE-MCD-561-0008), which states that "A detailed study of the sources of error w.r.t. astrometry leads to a relative accuracy of 50 μas over the full field in a single, well-calibrated exposure. This allows proper motion studies at the level of 40 μas/year for a single observing epoch and 10 μas/year for a 3-4 year campaign.", the requirements seem to be originating from "Call for Proposal For a Phase A Study of a High Angular Resolution Camera for the E-ELT, Specifications of the Instrument to be studied" (E-ESO-SPE-561-0097, v2.0), section 2.5.5, but in this document it is stated that "The final astrometry accuracy of the observations depends again both on stability of the AO module and of that of the camera. It shall be the task of the Consortium in the first phase of the study to extract from the science cases which require high astrometric accuracy the stability requirements and translate them into functional requirements for the hardware. ESO will coordinate the work of the Consortium studying the AO module with the one studying the camera to optimize the astrometric accuracy". Adherence to these requirements is proven in "High Precision Astrometry with MICADO", Trippe et al., MNRAS 2010.

Currently, the Top Level Requirements for ELT-CAM state the following requirements on the astrometric accuracy:

For an unresolved, unconfused source of optimal brightness in the centre of the field of view the relative position on the sky with respect to an optimal set of reference sources must be reproducible to within 50 μas (goal: 10 μas) over all timescales in the range of 1 hour to 5 years.

2.3 Iterate on the error budget for astrometry

Two error budgets are presented, although Trippe, in his paper, refers to Fritz et al. Trippe describes the error budget for MICADO on the E-ELT, while Fritz describes the error budget for astrometry for the VLT. GEMS is a facility instrument on Gemini, with the results of astrometric campaign described in Rigaut 2012 and Neichel 2012. Meyer 2011 describes the test measurements done on MAD.

Achieving
Full Astrometric Accuracy with MICADO
and Requirements for the MICADO ADC

Issue   1.0
Date   04.03.2013
Author   Remko Stuik
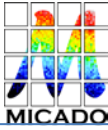
Error Term	Trippe (MICADO) μas	Fritz 2009 (8-10 m) μas
Sampling and pixel scales	1	
Instrument Distortions	30	130
Telescope Instabilities	0	
Achromatic Differential Atmospheric Distortion	1	
Chromatic Differential Atmospheric Distortion	20	10
Guide Star Measurement Errors	0	
Differential Tilt Jitter	10	15
Anisoplanatism	8	50
High-Z galaxies as reference sources	20	
Calibration of the projected pixel scale	10	30
Halo Noise	-	300
Confusion noise	-	100
SNR Induced position uncertainty	34	45
Extinction Uncertainty		10
Detector Non-linearity		<5

Table 1. Astrometric error budget for MICADO and a similar case on an 8-10 meter class telescope. Since the two error budgets come from different sources, not all terms exist in both. Halo Noise and Confusion noise are especially important in crowded fields and for now we have only considered isolated sources. Especially extinction uncertainty and detector non-linearity are not further described, but will need to be investigated. The SNR induced position uncertainty is the statistical error (photon noise). All other sources are described in the next sections.

Each of the error terms is described here below, and where possible extended for MICADO.

2.3.1   Sampling and pixel scales

The simulations as presented by Trippe and copied below seem to make sense, which means that under normal conditions, the sampling is not limiting the astrometric accuracy.
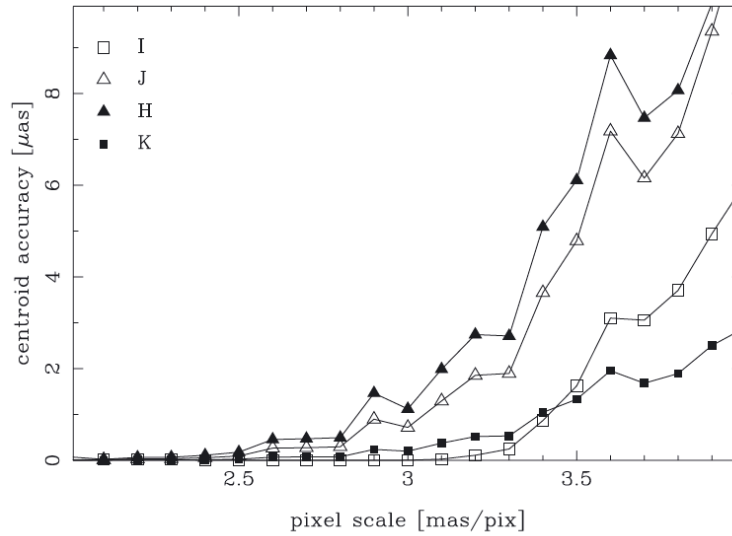
Figure 2. Pixel phase error versus pixel scale for *I, J, H, K* bands for *isolated* sources. Model PSFs are superpositions of Airy and Moffat profiles with Strehl ratios as given in Table 1. For all bands, the errors are below ≈ 1 μas for pixel scales smaller than 3 mas pix^{-1}.

2.3.2 Instrument Distortion

Trippe claims that for instrument distortions only the non-linear distortions are important as all linear distortions (shifts, rotations and linear scaling) can be calibrated out. The total distortions (linear + non-linear) is of the order of 0.3% of the Field of View (FoV). This corresponds to 0.16" on the 52" FoV of MICADO. Note that 50 μs corresponds to ~10^{-6}. Although looking at a local distortions at the scale of ~1" these distortions correspond to ~300 μas and only a factor of 10 needs to be gained by careful calibration. This does not take into account imperfections in the detector at the level of ~10 nm, corresponding to ~2 μas noise.

In general these distortions can be corrected for using a polynomial model and look-up tables. Three possible schemes are used, either separately or in combination:

1. Use parametric polynomial model for distortions
2. Use physical model of distortions. This is specifically useful for the largest part of the distortions introduced by the ADC as the system is rather well behaved.
3. Use look-up tables. For the HST this method has led to astrometric errors < 30 μas, although on-sky calibration on the E-ELT will be significantly harder due to the effects of the atmosphere and telescope stability. Initial calibration in a stabilized environment (In-lab/in-instrument) requires 40 nm knowledge of positions on the calibration mask to achieve 10 μas Accuracy. It also seems unlikely that calibrations can be performed on instrument in the unstable environment of E-ELT!

Several questions need to be answered: How accurate do you need to know plate scale variations over the field? In how far do they impact astrometry? Do we need to constraint the measurement sequence
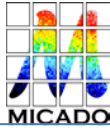
to always measure the same distances on the same location on the instrument? This will make measurements only possible with integer of 1 year in between, at least if there are time varying components in the your instrument distortion.

2.3.3   Telescope Instabilities

The E-ELT itself is also rather unstable. Although several loops are in use to ensure that the pointing and focus of the telescope are maintained, this does not guarantee plate scale. The expected plate scale variations are of the order of ~0.1%, or 60 mas. Furthermore, frame to frame rotations will cause again variations of the order of ~0.1%. These are predominantly linear coordinate transformations. Gravitational flexures are non-linear, but can in principle be corrected in same way as instrumental distortion, albeit without the presence of a calibration mask.

2.3.4   Differential Atmospheric Refraction

Both chromatic and achromatic differential atmospheric refraction are treated in the simulation section

2.3.5   Guide Star Measurement errors

Guide star measurement errors are important as the position of the GS varies as the atmosphere and zenith angle varies, which means that there is at least a variable offset to the field. Furthermore, in MCAO, since the positions of the multiple guide stars are not well known, these can introduce low-order distortions. In principle with N guide stars the distortions are of the order of N-1, so are in theory fully solvable with N-1 (2nd order) correction.

2.3.6   Differential Tilt Jitter

Measurement errors in the tilt measurements cause a residual jitter that is seen as position error in the science field. For a single star, this causes an error of 600 μas/crossing time (100s) or 50 μas ~4 hrs. For multiple guide stars this should further reduce and as integration time increases, the residual errors reduce as SQRT(t) and drop below ~10 μas after ~30 min (a factor 43!). The caveat is that this assumes a fully statistical differential tilt signal without any systematic or offset.

2.3.7   Anisoplanatism

Variation of shape of PSF versus position in field is an important effect and not well studied – the MAORY simulations as currently available are based on Fourier codes which, almost by definition produce too clean PSFs and were; the resulting PSFs show no tip-tilt components or asymmetries which are expected when doing adaptive optics. To first order there is only a Strehl degradation with isoplanatic angle, but due to the MCAO system, with multiple NGS in non-symmetric configurations, you also expect complex deformations of the field. The simulations done show MAORY PSFs in multiple field locations, where differences in offset due to the PSF are of the order of 7-8 μas. This is very likely a lower limit and needs to be investigated further. These investigations are currently taking place, but will not be known in the near future.

2.3.8   High-z galaxies

High-Z galaxies are used as an accurate, stable background reference frame to which to calibrate the astrometric offsets, especially in the absence of sufficiently bright (AB<23) stars. Galaxies are extended,

Achieving
Full Astrometric Accuracy with MICADO
and Requirements for the MICADO ADC

Issue 1.0
Date 04.03.2013
Author Remko Stuik
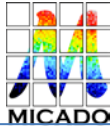
non-circular and sometimes have spectra which significantly deviate from stellar spectra (AGNs, dust, …) This can be partly mitigated by using unresolved star clusters in galaxies. The simulated galaxy fields that were used by Trippe require extremely long exposures and use point sources only. The accuracies achieved are 14-23 μas in 10 hrs or 29-65 μas/hr. An alternate technique using cross-correlations on extended sources (~4 μas for exposure times larger than 1 hour) seems promising, but cannot take into account rotations and scale factors, something which will become the most dominant error source.

Currently the definition of accurate reference source is an unsolved issue which will need to be solved.

2.3.9   Calibration of projected pixel scale

The 'final' step in the astrometric calibration is to translate the measured distances in pixels to a grid of known reference positions on the sky. This is not trivial; if for example the source positions over the full field of MICADO are known to 1 mas accuracy, this means that the error on scales of 0.5 arcseconds is still ~10 μas. This means that for an accurate mapping of the sources, their positions should be known with high accuracy. Currently only GAIA will produce a astrometric reference source catalogue which is sufficiently accurate.

2.4   Collect data required for simulations

2.4.1   ADCs studied and currently in use

According to the TMT ADC study [11], a state of the art ADC solution (2 counter rotating Amici prisms) results in a few miliarcseconds residual dispersion per wavelength band (at 65°), about 100 times worse than the current specification. Note that in order to compensate the effects of the ADC fully, not only the dispersion should be compensated, but also the atmospheric refraction itself, because this causes varying distortion in the field. In a 30 minute exposure this effect can be ~15 arcsec. Atad-Ettegui [12] focuses on concentrating the light in the diffraction spot, which is again 100 times worse performance than our specification. Yet even in this case a likely need for a closed-loop ADC control system is suggested, because of the (lack of) absolute accuracy of atmospheric dispersion predictions. A similar paper by Goncharov [13] compares the performance of a doublet, triplet and quadruplet ADC design. The performance is sufficient to reach the diffraction limit, but is nowhere near our specification. In the paper by Phillips [15], the performance of several ADC designs is investigated for several relevant bands.

In conclusion, there are several glass combinations that are capable of correcting atmospheric dispersion over zenith angles up to 65° to a level small than 1 milliarcsecond across the Z, Y, J, H, and K bands, no surprise so far. More important statement from the papers: The crossed-Amici prism design does not introduce image aberrations in a perfectly collimated beam, but is does introduce distortion. While the maximum distortion is under 1 mas, there are two obvious ramifications. First, for precision astrometry, this distortion will need to be calculated and removed. Secondly, a small amount of [field-dependent] image blur can occur as the elevation changes which could potentially limit exposure times.

From these papers we concluded that it is necessary to model the residual ADC effects (atmosphere + ADC) for realistic stars. The hope is that a normal ADC might just deliver the required performance

Achieving
Full Astrometric Accuracy with MICADO
and Requirements for the MICADO ADC

Issue   1.0
Date   04.03.2013
Author   Remko Stuik
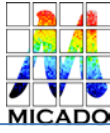
under ideal circumstances (long wavelength, very narrow band, similar stars, observe same field under similar conditions, e.g., exactly 1 year later at same ZD).

2.4.2   Atmospheric conditions and dispersion

The E-ELT site is Armazones, at latitude = -24.5893, longitude = 70.1917, altitude = 3064 m. The weather conditions have been extensively investigated and are available on the TMT Site characterization website. The standard weather conditions for Armazones are:

Parameter	Value
Temperature	6.5 °C
Pressure	712 mbar
Relative Humidity	22.0%

Table 2. Standard weather conditions for Armazones, as extracted from the median values on the TMT site characterization website.

This leads to the following uncorrected standard atmospheric dispersions:

	0°	30°	45°	60°
Broadband (0.580-2.58 µm	0 mas	383 mas	664 mas	1150 mas
I-band 0.72 – 0.92 µm	0 mas	59.9 mas	104 mas	180 mas
J-band 1.15 – 1.35 µm	0 mas	48.0 mas	27.7 mas	83.1 mas
H-band 1.50 – 1.70 µm	0 mas	18.0 mas	31.3 mas	54.1 mas
K-band 2.02 – 2.42 µm	0 mas	9.84 mas	17.0 mas	29.5 mas

Table 3. Overview of the computed uncorrected atmospheric dispersion for the standard atmospheric conditions, as described in Table 2, for the given filter bands .

2.4.3   Stellar Spectra

In order to determine the impact of the wavelength dependent dispersion on the position of a star in broad band filters, the displacement is convolved with the filter response and the stellar spectra. For the stellar spectra we use the Stellar Flux Library from Pickles [16]. For the filters we use I, J, H and K-band filter curves.

2.4.4   AO simulations

AO simulations were performed by the MAORY team for the MAORY Phase A study. The results of these simulations are available on the MAORY website.

2.4.5   ADC designs

Atmospheric diffraction is the effect of the atmosphere, acting as a prism with a wavelength dependent index of refraction. In general, this only causes a displacement in angle of the incoming wavefront with smaller higher order terms depending on the field of view. Atmospheric dispersion is the difference in atmospheric diffraction between wavelengths and causes a point source, like a star to look like an extended line on a broad band image. Both effects impact the astrometry and both effects are simulated.

Several types of ADC exist. For this study we investigate two types of ADC:

1. The ADC as described in the MICADO Phase A Opto-Mechanical design. This is a double set of counter-rotating prisms made up of ZnSe/ZnS. This ADC is located ~450 mm before the focus (of the telescope). In order to correct the optical errors caused by locating the ADC close to the image plane, two of the surfaces of the ADC have a small cylindrical curvature (~500 meter). In the rest of this document this ADC will be referred to as the image plane ADC

2. A similar set of ZnSe/ZnS counter rotating prisms located in a pupil plane, with the angles optimized for performance over 0.58 -2.58 micrometers. In the rest this of this document this ADC will be referred to as the pupil plane ADC.
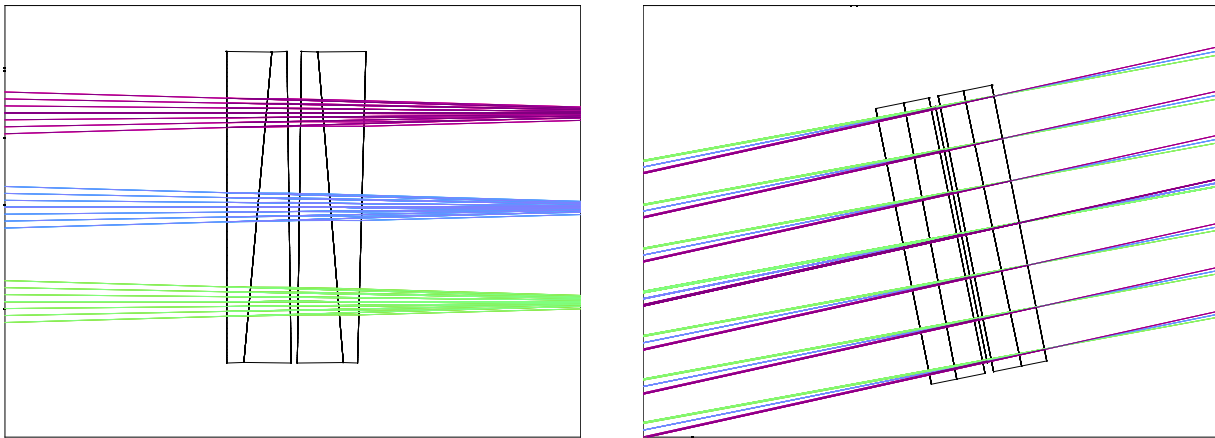
Figure 1. Layout of the two ADC concepts. Left the image plane ADC, located about half a meter before the first MICADO image plane. Right the pupil plane ADC, located at a pupil in the SCAO module or in the MAORY MCAO module.
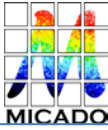
3 Simulations

3.1 AO Simulations

To be done – residual errors have been investigated for METIS.

3.2 Atmospheric Dispersion Simulations

The atmospheric dispersion simulations are based on two separate, but connected simulations:

1. ZEMAX was used to simulate the deviations of the chief rays[1] of the system under a variety of zenith angles[2] for the four main bands of MICADO: I, J, H and K-band[3]. Two different models, including E-ELT, MICADO and its SCAO system were used. The image plane ADC was located between SCAO and MICADO. The pupil plane ADC was located in the second pupil plane in the SCAO system. Note that this pupil plane might not be actually available[4].
2. Using the atmospheric data available from the TMT site characterization website, the deviations caused by the variations in atmospheric conditions are simulated.

As standard atmospheric conditions, the following parameters were used:

Parameter	Value
Site height	3064 meter
Median Temperature	279.65 K (6.5°C)
Median Pressure	712 mbar
Median Humidity	22%
Site Latitude	24.589° S
Reference day	1 July 2007

Table 4. Standard weather conditions for Armazones, as extracted from the median values on the TMT site characterization website. For investigating the effects for a real observation, a single reference day was selected to compute the astrometric errors as a function of time for 1 day.

For July 1st, temperature, pressure and humidity are given in Figure 2.

---

[1] Accurate simulations of the centroid position of the image on the detector to sub-micro arcsecond level accuracy, would require simulation of many, many rays. Since at this time we are not interested in the detailed effects of image quality on astrometry, we decided to only model the chief ray in order to speed up the simulations.

[2] At intervals of 5 degrees Zenith Distance from 0° to 60°

[3] All wavelength from 580nm to 2580nm are simulated at 0.5nm intervals.

[4] Pupil planes in AO modules are generally used to place Deformable Mirrors. If this is the case it is in principle possible to place an ADC just before a deformable mirror and use the ADC in double pass. There are some interesting challenges, like the incident angle on the ADC, etc. and he implications of such a setup have to be investigated.
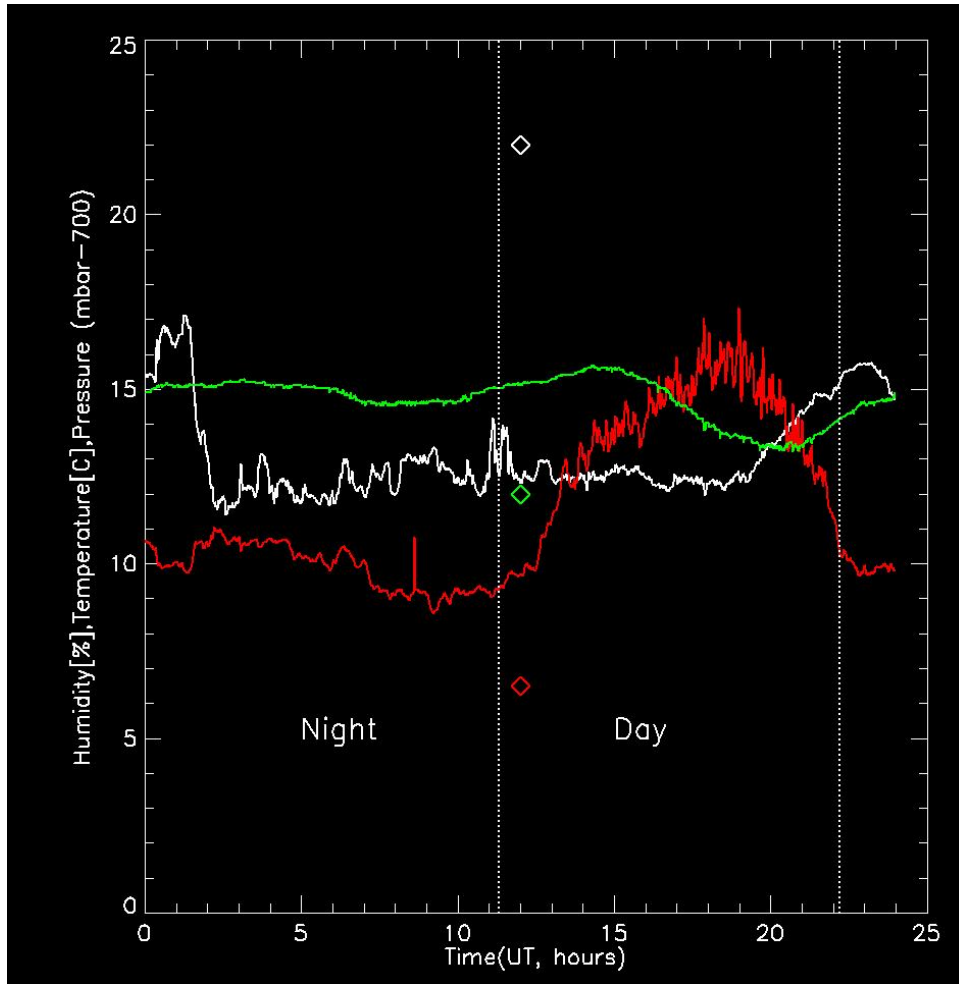
Figure 2. Temperature in °C (red), Humidity in % (white) and Pressure in mBar above 700mBar (green) for July 1st, 2007. Nigth time is from 0 to 11h19 (left) and day time is from 11h19m to 22h13m (right), time in UT.

Simulations on an ideal ADC were the following:

1. Image deformation as a function of Zenith Angle and wavelength
2. Image deformation as a function of ADC temperature and wavelength
3. Impact on astrometry of the color of stars under above deformation
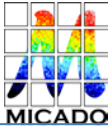
3.2.1 Image deformation as a function of Zenith angle

For each band the initial focusing was optimized for Zenith. For each Zenith angle, the position of the ADC was optimized to minimize size of the chromatic PSF. This immediately means that the ADC rotation angle varied from band to band. The following ADC rotation angles were used:

Zenith Distance (degree)	Image Plane ADC Angle (degree)				Pupil Plane ADC Angle (degree)			
	I	J	H	K	I	J	H	K
0	0.00	0.00	0.00	0.00	0.00	0.00	0.00	0.00
5	-2.13	-2.86	-3.33	-4.93	-1.92	-2.58	-3.04	-6.33
10	-4.29	-5.76	-6.73	-10.01	-3.88	-5.21	-6.13	-12.83
15	-6.52	-8.78	-10.26	-15.43	-5.90	-7.94	-9.35	-19.72
20	-8.87	-11.96	-14.01	-21.46	-8.03	-10.81	-12.74	-27.28
25	-11.40	-15.40	-18.08	-28.51	-10.31	-13.90	-16.41	-35.96
30	-14.16	-19.20	-22.61	-37.45	-12.79	-17.30	-20.47	-46.63
35	-17.26	-23.50	-27.83	-50.66	-15.58	-21.14	-25.10	-61.82
40	-20.82	-28.55	-34.07	-92.78	-18.77	-25.60	-30.54	-90.05
45	-25.04	-34.71	-41.99	-90.35	-22.54	-30.98	-37.26	-90.01
50	-30.28	-42.74	-53.09	-90.16	-27.17	-37.82	-46.15	-90.01
55	-37.13	-54.41	-74.30	-90.10	-33.15	-47.26	-59.73	-90.00
60	-46.97	-80.49	-90.04	-90.07	-41.49	-62.84	-90.01	-90.00

Table 5. Overview of the zenith distance and corresponding optimal ADC rotation angle for that zenith angle and band. Note that the K-band ADC angle saturates at a zenith angle of ~45. This is due to the optimization process for this specific ADC, done for the full band from 0.58 to 2.58 µm, leaving some residual errors at K-band for larger zenith angles.

For each of the Zenith angles and bands, the distance is measured between 8 points at the edge of the field of view of MICADO and in the image center. The results are compared with respect to the distance measured at Zenith. The residuals are considered the astrometric offsets and plotted in Figure 3 to Figure 5. Figure 3 shows the large scale structure of the astrometric offsets. For an ideal ADC, these offsets can be either computed or calibrated with high accuracy and should not lead to an increase in the astrometric error, as long as interactions with other error terms are minimized. Figure 4 zooms in on the lower right corner of these plots for each zenith angle, subtracting the average differential distance for each band. If the wavelength dependence of the intensity of the source is known, this still does not contribute to the astrometric error as this is still a deterministic error. Figure 5 shows the residual astrometric offsets when convolving with the 41 K- and M-star spectra. If the stellar type is not known, these are real astrometric errors (although by measuring at several zenith angles, this error can probably be reduced).

Achieving
Full Astrometric Accuracy with MICADO
and Requirements for the MICADO ADC

Issue   1.0
Date   04.03.2013
Author   Remko Stuik

3.2.2   Simulation plots

	Image Plane ADC	Pupil Plane ADC
I	Scale = $1 \cdot 10^5$ micro arcsecond	Scale = $2 \cdot 10^4$ micro arcsecond
J		

Image Plane ADC	Pupil Plane ADC
H	
K	
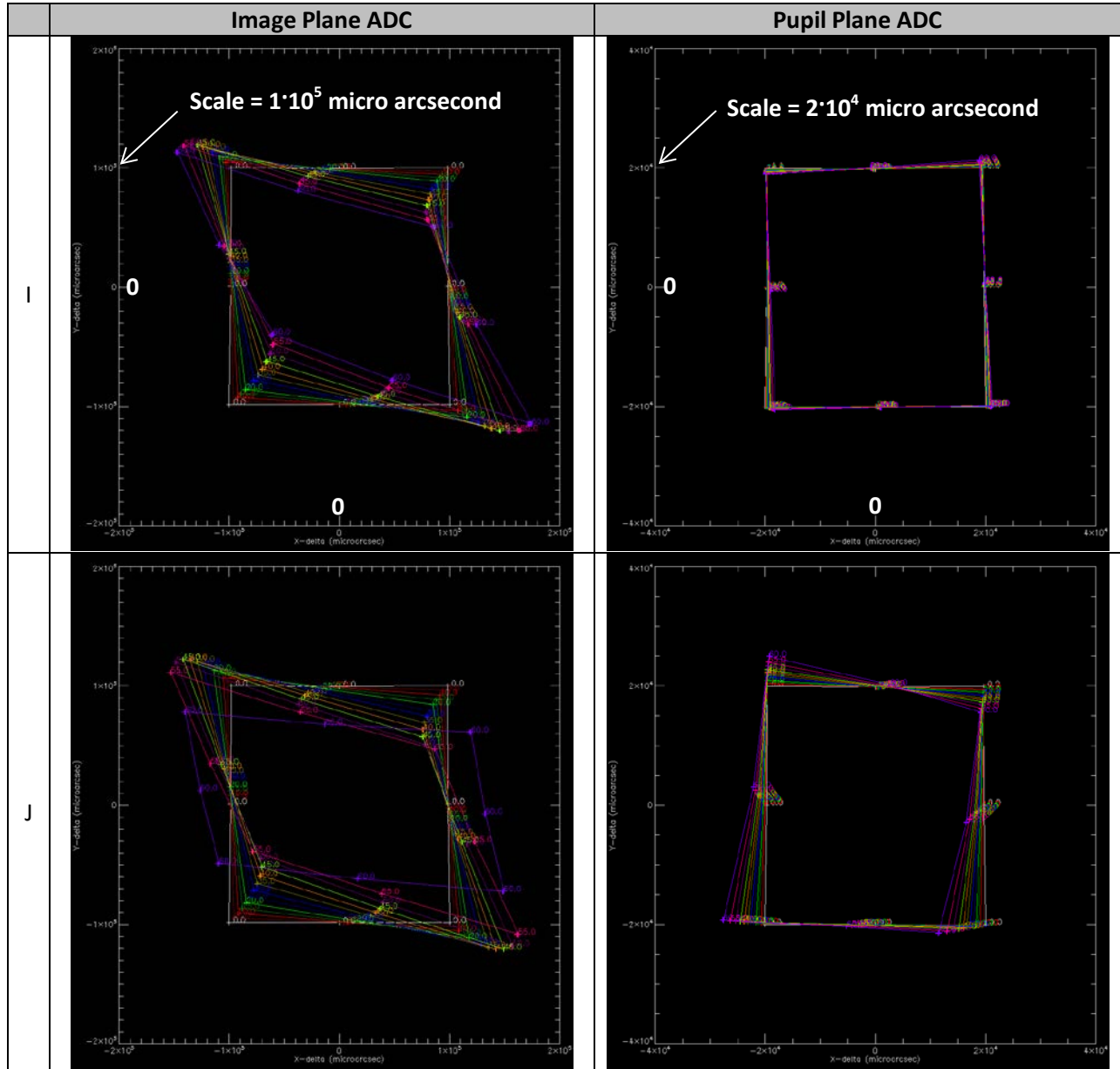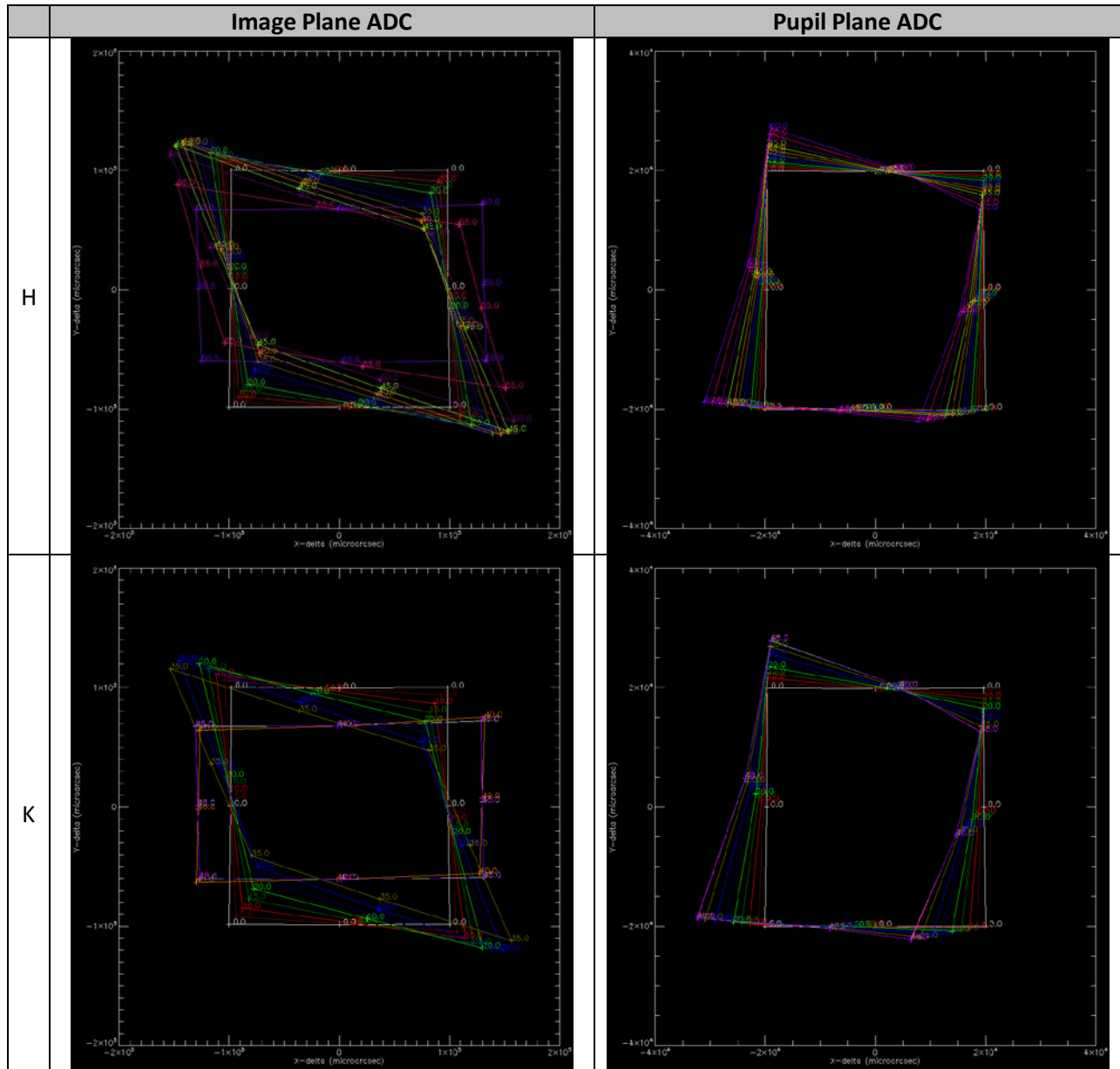
Figure 3. In the above 8 plots the difference in distance between image center and 8 edge of the MICADO field points are shown. What is shown is the relative distance variation between these points at zenith distance of 0 and given zenith distance (up to 60 degrees, given by different colors). For reference, the zero-position is given as a square, i.e., the distortion at the upper left corner for I-band at 60 degrees is Δx = -5000, Δx = +1000 with respect to the center position. From top to bottom the different bands are shown: I, J, H and K-band. The plots at the left are for an image plane ADC, the plots at the right for a pupil plane ADC. Notice the difference in scale! The scale is 1·10^5 for the Image plane ADC, which is five times larger than the scale of 2·10^4 for the Pupil plane ADC. The points on the square are the renormalized field positions. The distortions increase if the Zenith Distance increases. Distortions are expected to be low order, but are more complex than just a field rotation and magnification in X and Y.

Achieving
Full Astrometric Accuracy with MICADO
and Requirements for the MICADO ADC

Issue 1.0
Date 04.03.2013
Author Remko Stuik

Image Plane ADC	Pupil Plane ADC

I

ZD=0° ZD=5° ZD=10° ZD=15°

ZD=20° ZD=25° ZD=30° ZD=35°

ZD=40° ZD=45° ZD=50° ZD=55°

ZD=60°

Scale = 400 micro arcsecond

Scale = 200 micro arcsecond

J
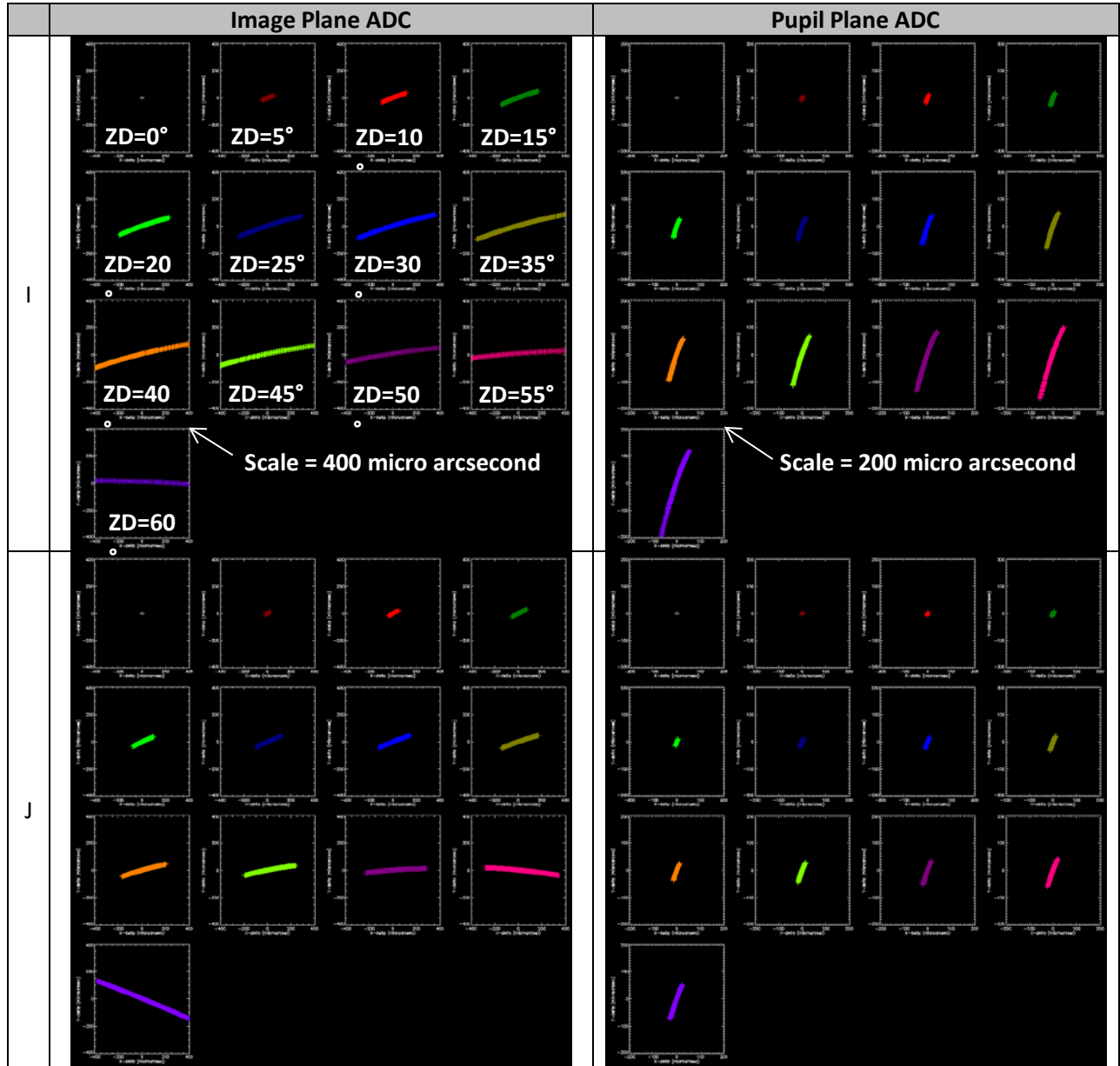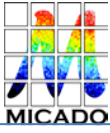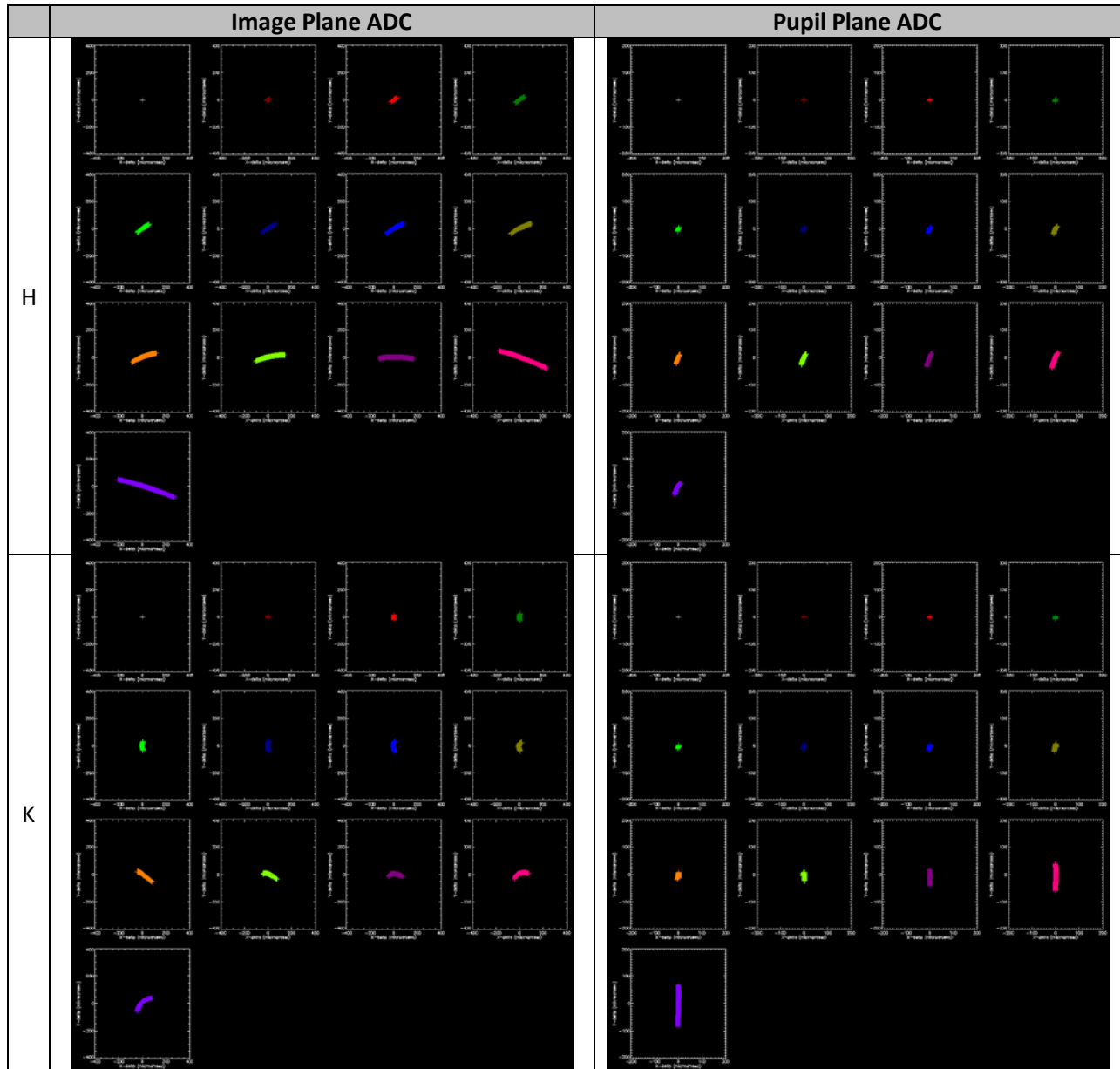
Figure 4. The layout of the 8 plots above is similar as in figure 3: From top to bottom the different bands are shown: I, J, H and K-band. Left is for the image plane ADC, right for the pupil plane ADC. In the above 8 plots the residual chromatic error is shown for one of the points at the edge of the MICADO field. The residual chromatic error is the wavelength dependent distance between center and corner point. What is shown in the 13 sub-plots is the difference between the effect a zenith distance of 0 and given zenith distance from 0 up to 60 degrees at 5 degree interval. Each point indicates the position of a different wavelength within the band, creating a line or curve. Notice the difference in scale! The scale is 400 for the Image plane ADC, which is twice as large than the scale of 200 for the Pupil plane ADC.

Achieving
Full Astrometric Accuracy with MICADO
and Requirements for the MICADO ADC

Issue   1.0
Date   04.03.2013
Author   Remko Stuik

	Image Plane ADC	Pupil Plane ADC
I	ZD=0° ZD=5° ZD=10 ZD=15° ZD=20 ZD=25° ZD=30 ZD=35° ZD=40 ZD=45° ZD=50 ZD=55° ZD=60 Scale = 200 micro arcsecond	Scale = 20 micro arcsecond
J	Scale = 200 micro arcsecond	Scale = 20 micro arcsecond
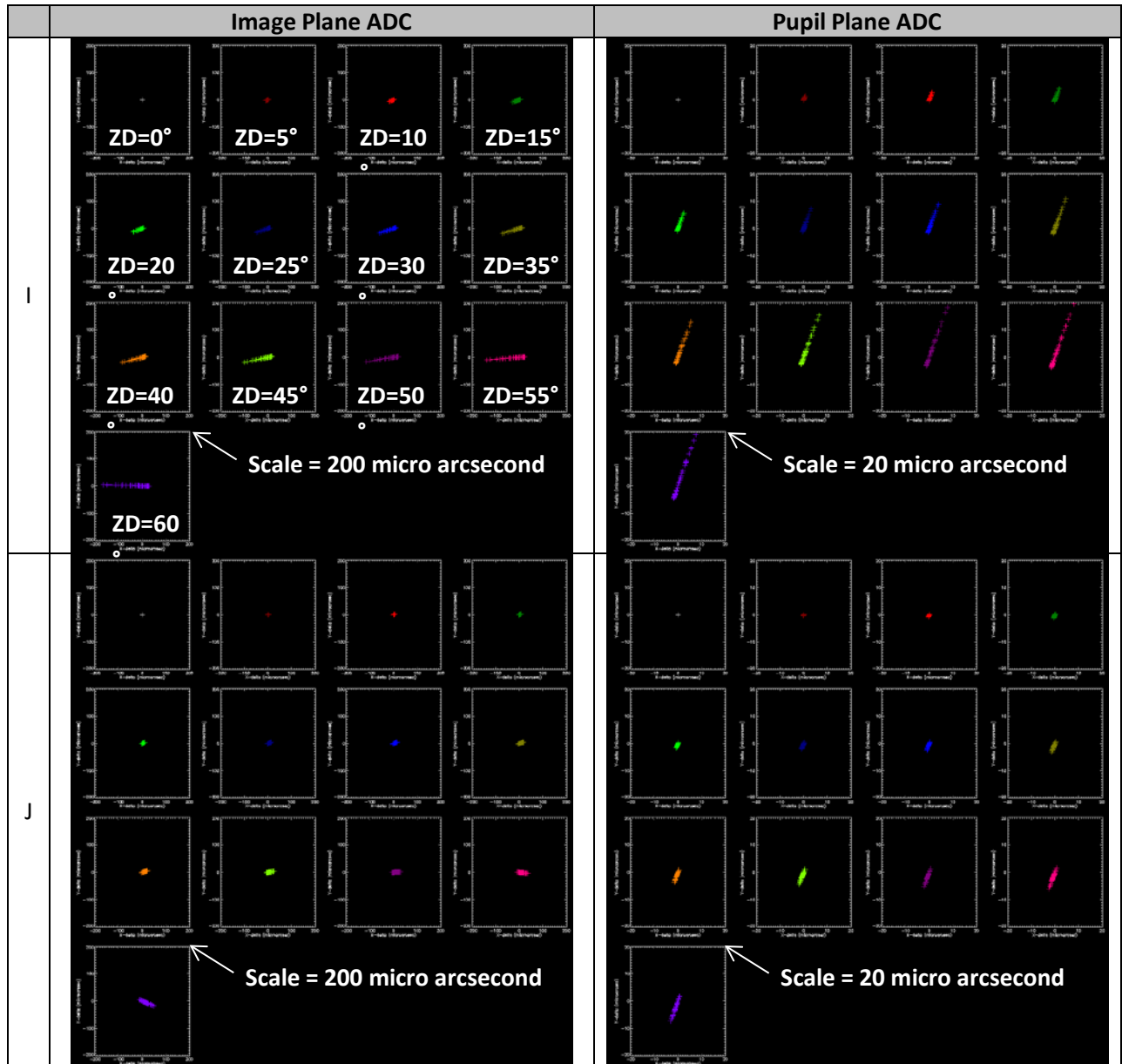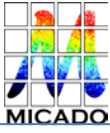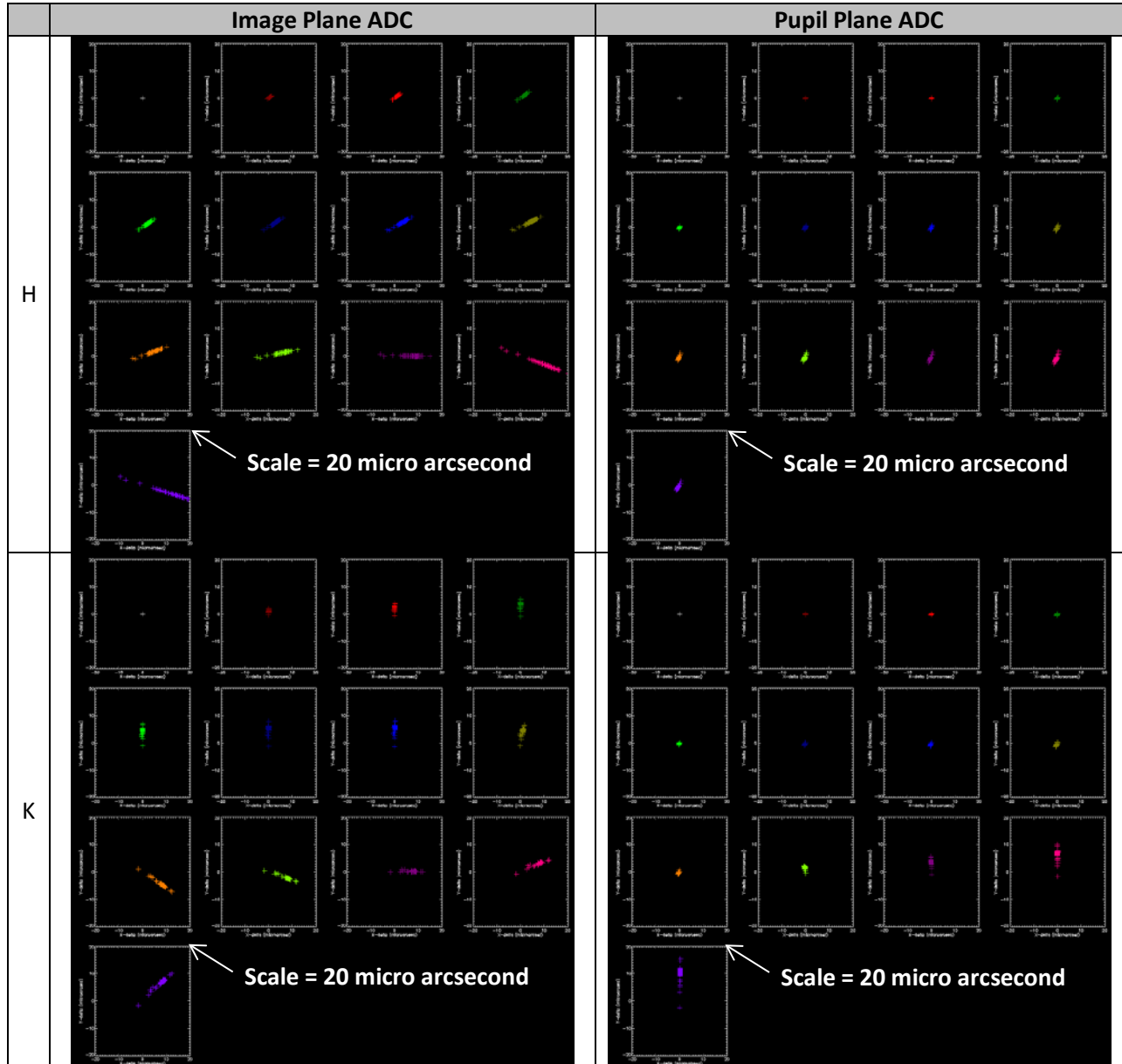
Figure 5. The layout of the 8 plots above is similar as in figure 4: From top to bottom the different bands are shown: I, J, H and K-band. Left is for the image plane ADC, right for the pupil plane ADC. The residual chromatic error is shown for one of the points at the edge of the MICADO field is shown for different stellar types. Each cross indicates a different stellar type. Notice the difference in scale! The scale is 200 micro arcseconds for the Image plane ADC in I-band and J-band, which is ten times larger than the scale of 20 micro arcseconds for the Pupil plane ADC and the scale for the Image plane ADC in H-band and K-band.
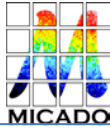
3.2.3 Simulation Results Discussion and Conclusions

From Figure 3 it can be concluded that any ADC, either in the pupil plane or in the image plane, causes distortions in the image plane. The size of these distortions is up to 5 or 50 mas, depending on the chosen ADC type. The pupil plane ADC results in significant lower distortions, compared to the image plane ADC. The distortions are relatively low-order, but more than simply a Rotation + Magnification in X and Y. With proper physical modeling of the instrument, these ADC induced distortion can be largely corrected for.

The E-ELT diffraction limit ranges from ~4.5 mas at I-band to ~15 mas at K-band. MICADO exposure durations are in the order of a minute. In this timeframe the distortions vary to ~0.2 mas for the image plane ADC and ~0.02 mas for the pupil plane ADC. Therefore no noticeable consequences for imaging contrast or the sensitivity of MICADO are expected, regardless of the ADC type.

However the distortion is significant if multiple exposures are taken from the same field. This means that the fields cannot be simply added without impacting the imaging contrast. Arguably this could be acceptable for photometry only in case of a pupil plane ADC and limited exposure time =limited ADC movement.

From Figure 4 it can be concluded that the residual chromatic dispersion within a band is in the order of magnitude of 100 micro arcseconds at relevant Zenith Distances. The largest effect[5] is 300 micro arcseconds at 60°ZD for the pupil plane ADC and more than 1 mili arcsecond for the image plane ADC. Again, this performance seems acceptable for imaging: in nearly all cases the sensitivity is hardly affected.

However for accurate astrometry the residual chromatic dispersion within a band could be noticeable due to the spectral differences between stars. In Figure 5 these effects are shown to be up to 200 micro arcsecond for the image plane ADC and up to 20 micro arc second for the pupil plane ADC.

Conclusion: For accurate astrometry knowledge the spectral type is required in order to de-convolve the residual chromatic dispersion from the stellar types in the general case. However, in best cases (H and K band at low ZD and pupil plane ADC and averaging over multiple observations at different Zenith Distance) we might be able to do without this step.

---

[5] At 60°ZD at the very edge of the MICADO field for the I-band. The effect might be noticeably larger in case a broadband filter I+J band is used.

Achieving
Full Astrometric Accuracy with MICADO
and Requirements for the MICADO ADC

Issue   1.0
Date   04.03.2013
Author   Remko Stuik
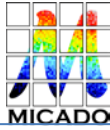
3.2.4   Image deformation as a function of Temperature

As part of the ZEMAX simulations, also the temperature of the ADC was varied. Note that for the purpose of this study *only* the temperature of the ADC was varied, but that the rest of MICADO, SCAO and E-ELT were considered not to change temperature. The temperature was changed by ±5K and ±0.01K to represent respectively an ADC at in atmospheric environment with temperature fluctuations and a temperature stabilized ADC in a vacuum system. No temperature gradients or differential temperatures in or between materials were taken into account at this time.

The results are shown in Figure 6. In most cases, only the nominal and large temperature variations are visible as the curves of the temperature stabilized ADC overlap with the nominal case. Each figure represents a single band and ADC type. Each panel within each figure corresponds to a certain Zenith distance, varying from 0 in the top left to 60 degrees in the lower right in 5 degree intervals. Figures on the left are for the image plane ADC, on the right for the pupil plane ADC.

Achieving
Full Astrometric Accuracy with MICADO
and Requirements for the MICADO ADC

Issue   1.0
Date   04.03.2013
Author   Remko Stuik

Image Plane ADC	Pupil Plane ADC
I	ZD=0° ZD=5° ZD=10° ZD=15° ZD=20° ZD=25° ZD=30° ZD=35° ZD=40° ZD=45° ZD=50° ZD=55° ZD=60° Scale = 200 micro arcsecond	Scale = 200 micro arcsecond
J		

Achieving
Full Astrometric Accuracy with MICADO
and Requirements for the MICADO ADC

Issue   1.0
Date   04.03.2013
Author   Remko Stuik
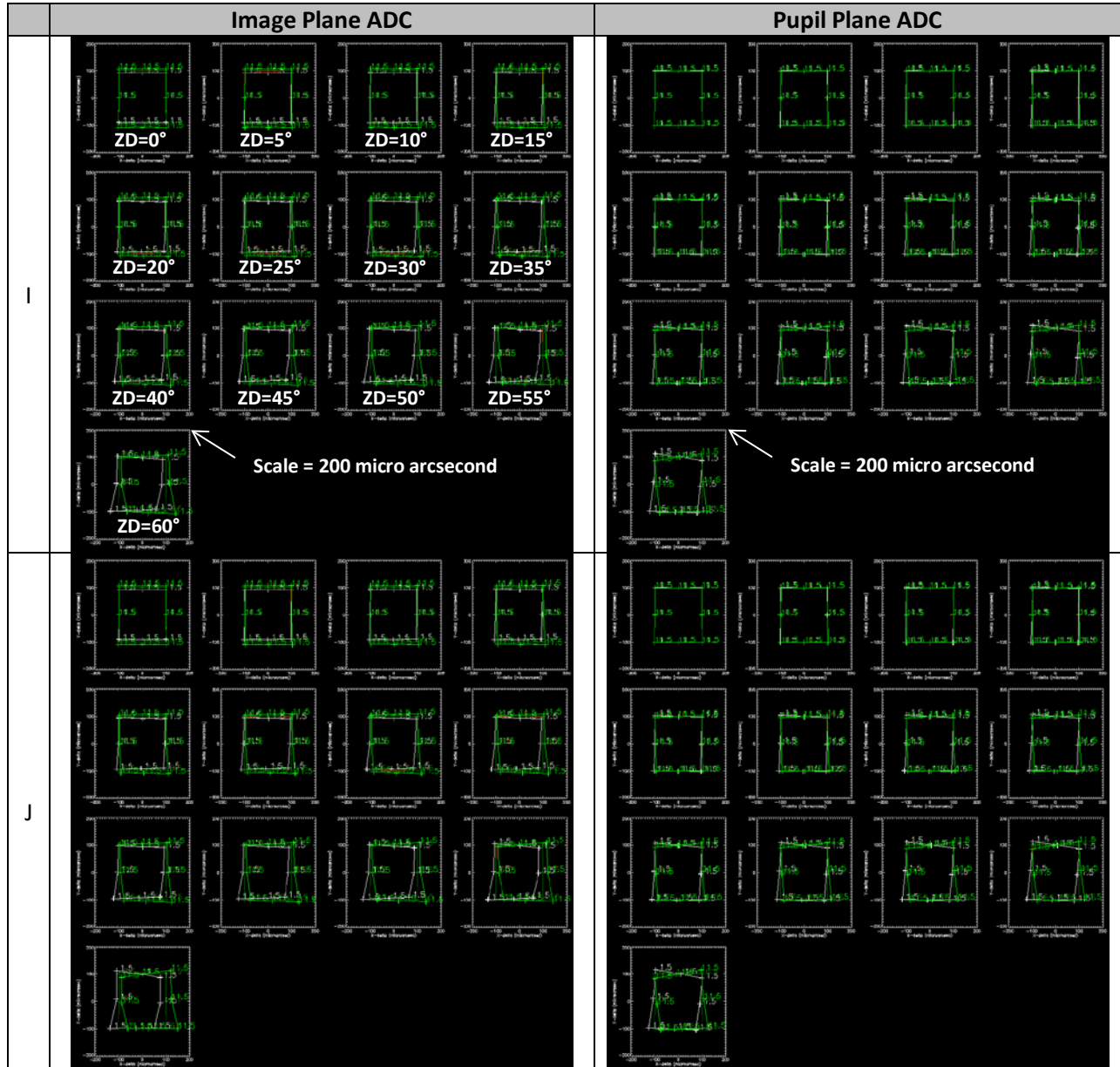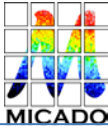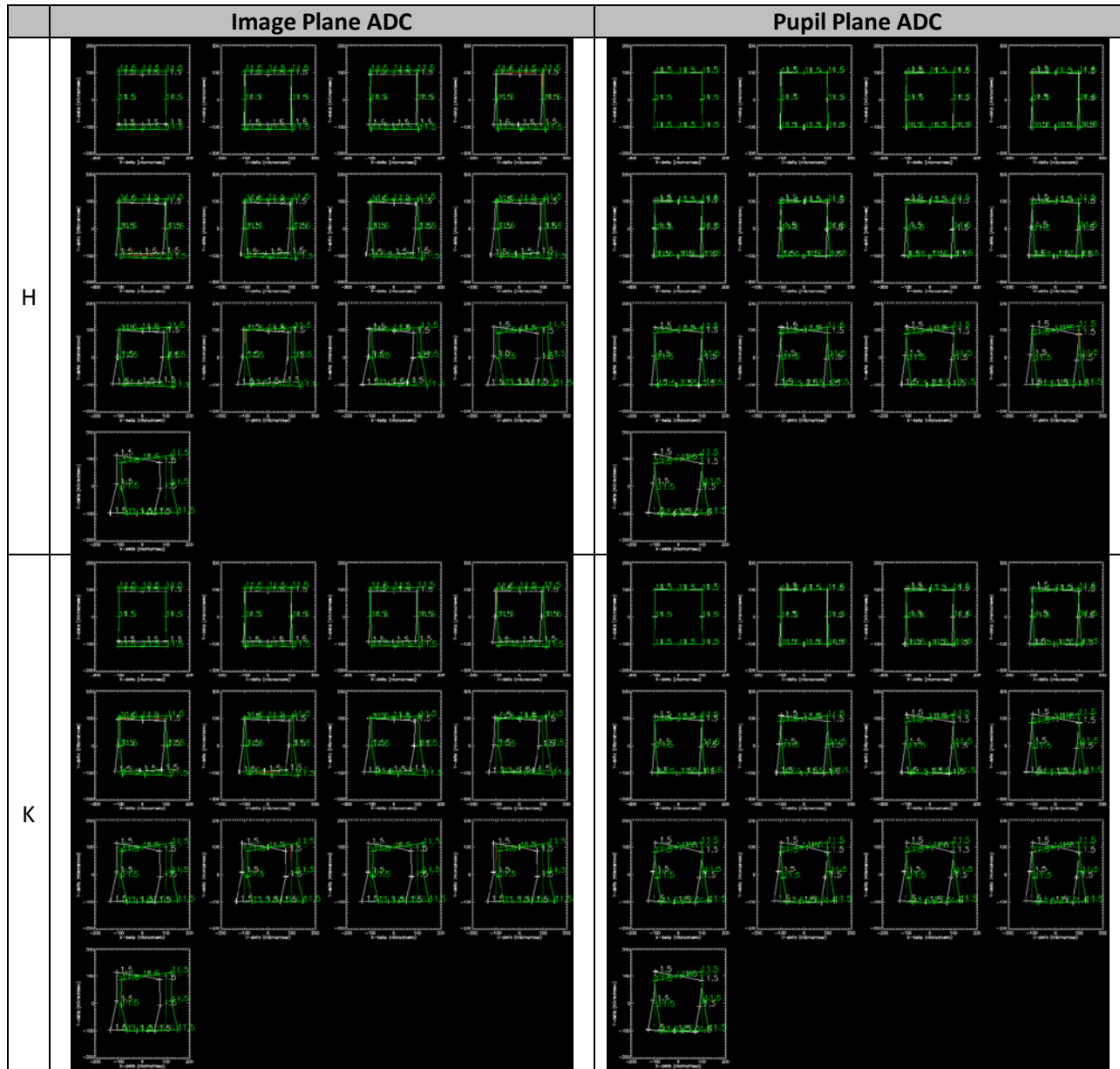
Figure 6. Impact of temperature on the astrometric precision. 5 conditions were investigated; nominal (6.5°C) ±5K (nominal temperature variations on Armazones) and ±0.01K (temperature stabilized ADC). In most cases, only the nominal and large temperature variations are visible as the curves of the temperature stabilized ADC overlap with the nominal case. Each figure represents a single band and ADC type. Each panel within each figure corresponds to a certain Zenith distance, varying from 0 in the top left to 60 degrees in the lower right in 5 degree intervals. Figures on the left are for the image plane ADC, on the right for the pupil plane ADC.

Although not plotted here, the residual chromatic component is of the order of 1 uas or less under all conditions. No knowledge regarding the spectrum is required to obtain the desired astrometric accuracy.

In conclusion, the maximum expected variations for un-stabilized temperature ADC (albeit uniform in temperature) is of the order of 100 µas (peak-peak / 1.5°C-11.5°C) (→ ~10 µas/K). With a temperature

stabilized ADC (+/- 10mK) the resulting variations are at a level of a sub-micro arcsecond astrometric under almost all conditions. The pupil plane ADC shows slightly less and slightly less higher-order distortions than the image plane ADC.

From Figure 2, a temperature variation over a night of ~2 degrees does seem to be a reasonable assumption. At this level, at least partial stabilization would be required to remove astrometric errors due to temperature fluctuations, although temperature stabilization to ~0.1 K seems to be sufficient to reach micro arcsecond accuracy.

Alternatively the distortions could be calculated in a physical model using the measured temperature data of the ADC. In this case further investigations are necessary using dynamical temperature models of the ADC and the surrounding area.

3.2.5 Impact of variations in the atmosphere

The TMT site characterization website has a large database on the climatology of Armazones. The atmospheric dispersion is to good approximation determined by the temperature, pressure and humidity at the telescope site (with larger deviations taking place for larger zenith distances). A single day was chosen and the variations in the astrometry due to variations in temperature, pressure and humidity. The results are shown in the three panels in Figure 7 for a zenith distance of 45°. The left plot is the difference in position between a point in the center and at the edge. Note that the plot shows a range in wavelength for I (white), J (red), H (green) and K (blue) bands. In the middle plot, for each wavelength band the displacement for the shortest wavelength was subtracted. In right plot the displacements are convolved with 41 stellar spectra of K- and M-stars. Note that extending this plot to O-stars does increase the spread of the curves slightly, but not by a significant amount.
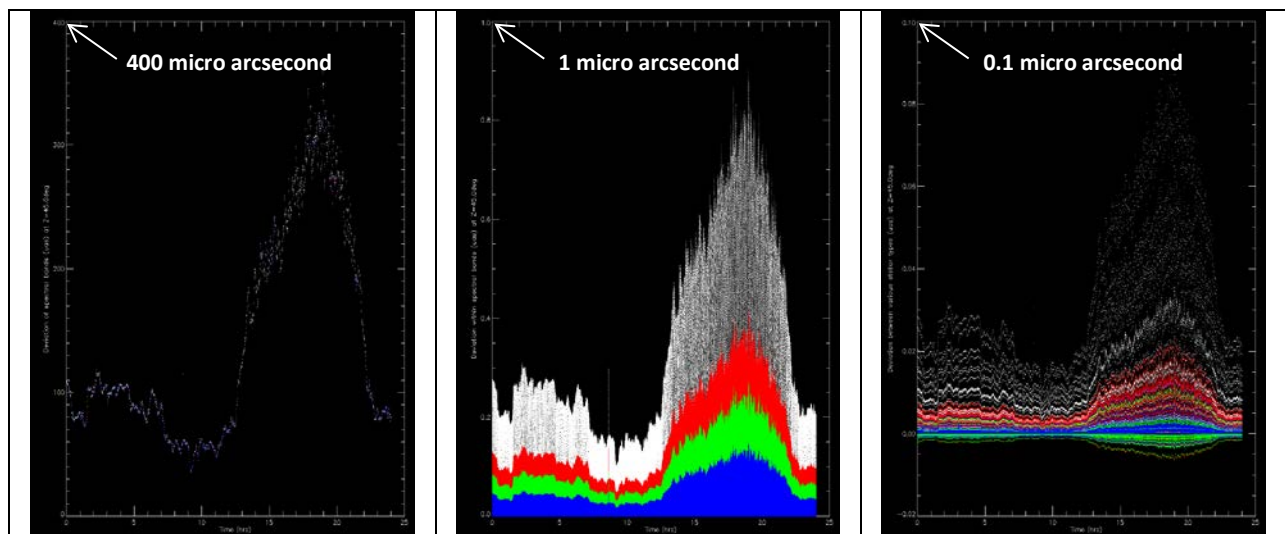
Figure 7. Three curves, demonstrating the temporal variations in the relative astrometry for a zenith angle of 45 degrees. The left plot is the difference in position between a point in the center and at the edge. Note that the plot shows a range in wavelength for I (white), J (red), H (green) and K (blue) bands. In the middle plot, for each wavelength band the displacement for the shortest wavelength was subtracted. In right plot the displacements are convolved with 41 stellar spectra of K- and M-stars.
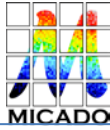
When optimally tuned, the maximum uncorrected dispersion for I-band to K-band at 60 degree zenith angle ranges from 180 mas to 30 mas respectively. Index of refraction variations due to temperature, pressure and humidity fluctuations, as seen in the TMT site characterization for Armazones, stay within a band of 2%, i.e., the maximum deviation is of the order of 1%, giving rise to a maximum dispersion error due to the atmospheric fluctuations of 1800 – 300 μas for I-band to K-band. During a night, these fluctuations are significantly smaller, as seen in the Figure 2. The resulting variations in the temperature, pressure and humidity can cause astrometric errors at the level of ~50 μas over a night by changing the plate scale in the altitude direction. There are two ways to deal with this effect. On the one hand, this effect can be calibrated, although this will make that again image stacking is not directly possible. A second method is by accurately monitoring the temperature, pressure and to a lesser extend humidity. For K-band the required accuracy is better than 0.03%, or 0.1°C and 0.2 mbar. For I-band these requirements are a factor 6 tighter and become very hard to measure as local temperature and pressure variations start to impact the measurements significantly.

The impact of chromatic errors is minimal, increasing the spot by less than 1 μas and no knowledge regarding stellar types is required to compensate for variations in the climatological conditions.

3.2.6   Impact of the imperfections in the ADC

Just like the rest of MICADO, manufacturing errors in the ADC are unavoidable. But where the rest of MICADO is not moving[6], by nature, the ADC needs to rotate and any errors in the manufacturing will cause time-varying errors. In this section we describe the impact of the various error sources in the ADC. For this analysis we assume the current pupil plane ADC. The optical prescription of this ADC is:

Name	Thickness (mm)	Material	Diameter (mm)	Tilt around X (degree)
Surface 1A	30	ZnSe	310	0.0000
Surface 1B	30	ZnS	310	0.5649
Surface 1C	10	Air	310	-0.0905
Surface 2A	30	ZnSe	310	0.0548
Surface 2B	30	ZnS	310	-0.5100
Surface 2C	-65	Air	310	0.1453

Table 6. Overview of the optical properties of the surfaces of the pupil plane ADC. (The image plane ADC is described in the MICADO Opto-Mechanical Design report).

The following errors could occur:

1. Errors in the index of refraction of the materials. Inhomogeneities in the index of refraction of the blanks are described by the ISO 10110/part 4 classification . Assuming a classification of 'h4',

---

[6] In the Phase A study of MICADO it was a deliberate choice to hold MICADO completely static with respect to the stellar field under observation. Distortions and imperfections in the optics are then static to the detector and easy to calibrate. The entire instrument co-rotates with the starfield over a vertical axis to avoid flexure induced variations in the MICADO instrument.

Achieving
Full Astrometric Accuracy with MICADO
and Requirements for the MICADO ADC

Issue   1.0
Date   04.03.2013
Author   Remko Stuik
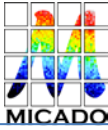
which indicates a maximum inhomogeneity of 1×10^{-6} will for the given blank thickness of 120 mm, lead to a PtV surface error of 120 nm per set of two prisms, or ~24 nm RMS.

2. Errors in the tilt of each of the 6 surfaces that make up the ADC. A typical tolerance on the thickness is of the order of 10".

3. Surface errors on each of the 6 surfaces. Typical surface errors that can be obtained for these surfaces are l/10 PtV at 632 nm, so of the order of 15 nm RMS per surface, or ~25 nm RMS for each of the prisms.

4. Tilt and offset of the rotation axis of the two sets of prisms. Alignment of the axis can be done to better than <10" in angle and 20 microns in lateral displacement.

5. Errors in the tracking/offset from ideal rotation of the prisms. The tracking should be accurate to better than 10", i.e. ~0.003 degrees.

No time was available for a full sensitivity analysis, but a 100-realizations Monte-Carlo simulation was performed, taking into account the surface errors, the errors in the tilt of the surfaces of the prisms and a static offset in the ADC rotation angle, all with a magnitude as given in the previous paragraph. The results are shown in Figure 8.
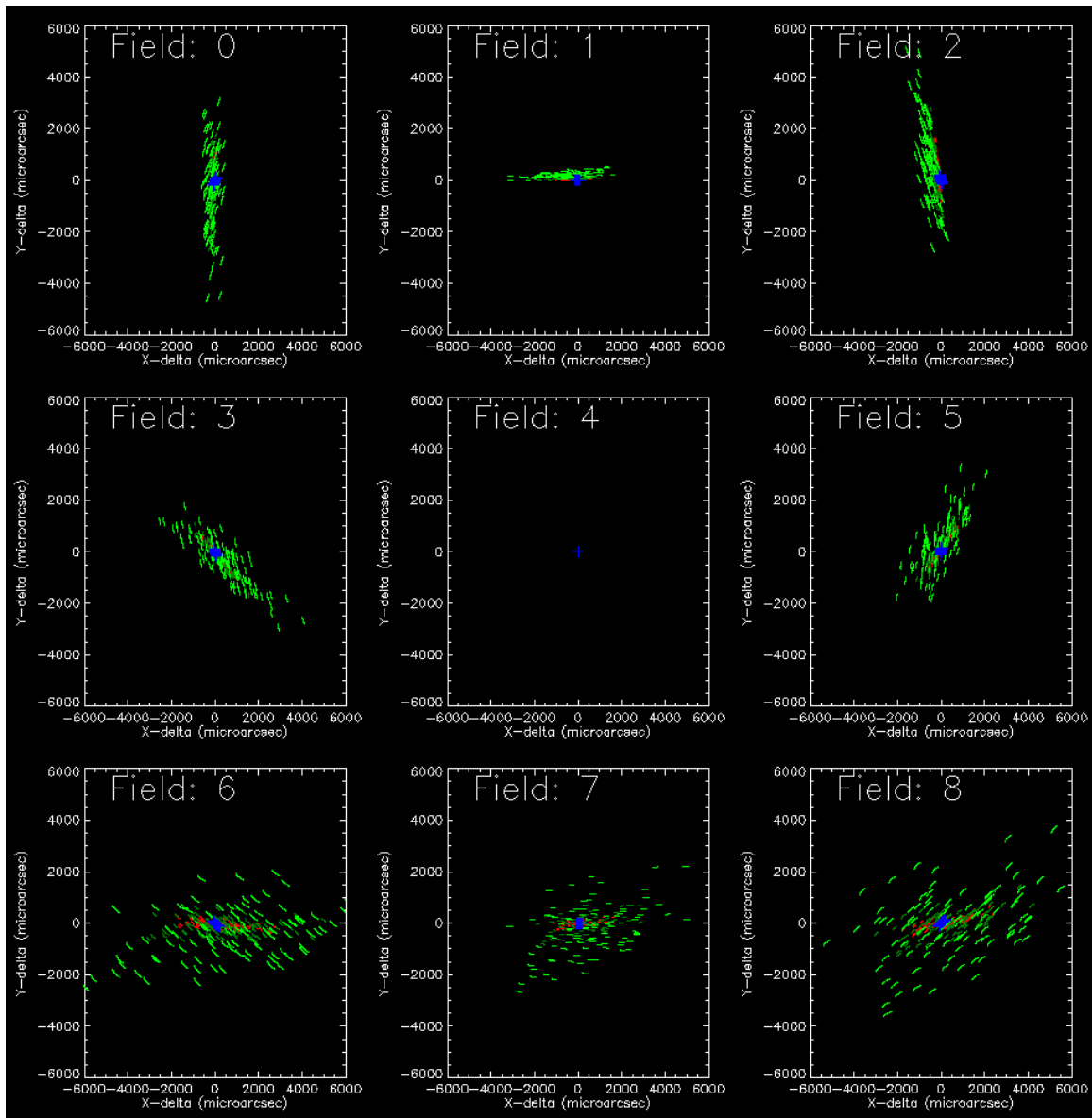
Figure 8. Relative offset of a point in the field (indicated by the 9 panels) and the central position for the I-band, for zenith angles of 0, 15, 30, 45 and 60 degrees (white, dark red, light red, dark green and red green respectively). Each dot is a point in wavelength, with a series of 200 dots making up the full I-band. The lines are therefore an indication of the spectral spread. The blue crosses indicate performance of the 'perfect' ADC.

Figure 8 shows that the main impact of an imperfect ADC is a non-linear, likely non-uniform scaling of the image. From the figure it can be seen that the spectral dispersion is a second order effect, as all the spectral line segments have the same shape, regardless of the distortion. The PSF of the stars is not spread significantly within the band, so the effect on the imaging performance is small.
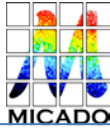
4 Conclusions

4.1 Top Level Requirements for E-ELT-Cam

Returning to the official top level science requirements for MICADO:

"For an unresolved, unconfused source of optimal brightness in the centre of the field of view the relative position on the sky with respect to an optimal set of reference sources must be reproducible to within 50 µas (goal: 10 µas) over all timescales in the range of 1 hour to 5 years."

From the results of this study the following restrictions could be noted for astrometric observations:

1. Avoid I band
2. Avoid Zenith Angles > ~45 degrees
3. Avoid trying to achieve the most accurate astrometry over the full field

Note: In the simulations the results are a factor 2-3 too optimistic since distances to the image center are measured rather than from corner to corner, which in most cases makes errors seem equivalently smaller.

4.2 ADC requirements to meet science requirements

From the results of this study it can be concluded that:

1. There is a strong preference to locate the ADC in the pupil plane. The astrometric performance, especially when insufficient information is available on stellar type, is much better than an image plane ADC
2. There is a strong preference for the ADC to be temperature stabilized. Likely ~0.1K is sufficient.
3. Preliminary indications are that errors in the ADC, like the wavefront errors and errors in the tilts of the surfaces do have a significant impact on the astrometry. The largest component is in an overall shift of the field, but significant errors in the relative astrometric solution can be seen. For the moment, these errors are in a range which can still be corrected by calibration, but further investigation (and maybe tightening of the requirements) is required.
4. Even the best ADC will not be able to reach the astrometric accuracy without a) a good calibration, b) active feedback and c) a posteriori corrective van de astrometric solution.

Achieving
Full Astrometric Accuracy with MICADO
and Requirements for the MICADO ADC

Issue 1.0
Date 04.03.2013
Author Remko Stuik

5 Draft Operational Strategy

The draft operational strategy is explained in Figure 8.
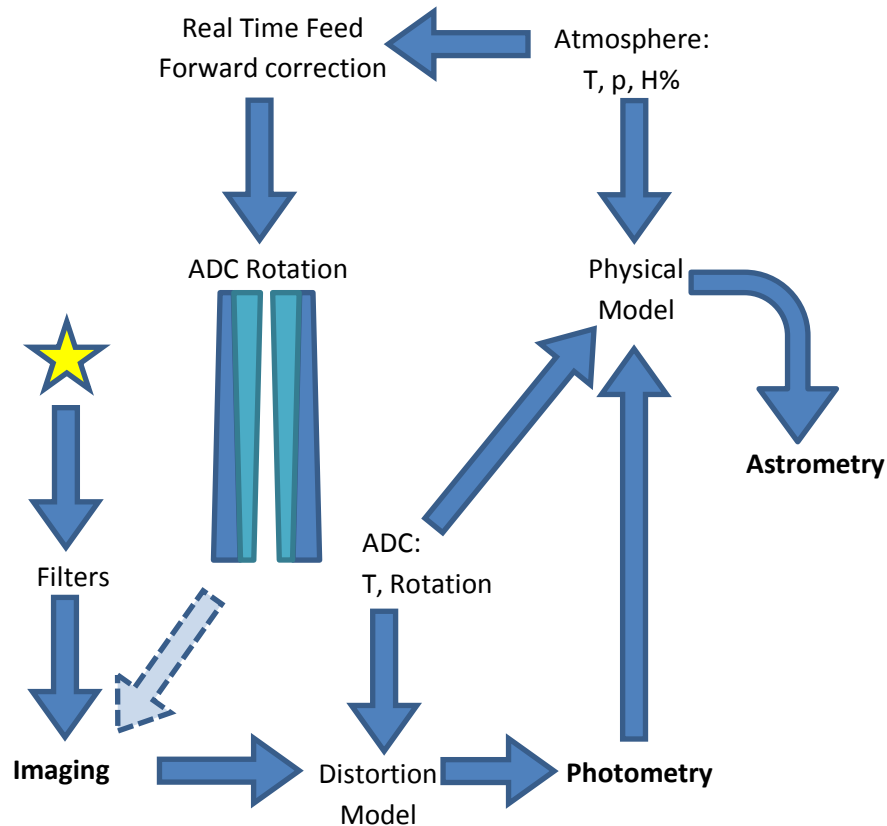
Figure 9. Schematic overview of the operational strategy. The atmospheric parameters are used to correct the ADC rotation real time using a feed forward correction. This is to keep the residual spectra below the 1 miliarcsecond level at all times, in order to meet imaging requirements. The ADC temperature and rotation are monitored and stored in the FITS file. When stacking multiple images for Photometry, the ADC status information is used in an offline distortion model. For optimal astrometry first the star type of each object must be determined using photometry with at least 2 filters. The atmospheric parameters are also stored in the FITS file. The atmospheric data, the ADC data and the star type are used together in an offline physical model of the entire system to generate detailed distortion corrections for each star.

The operational strategy is developed, keeping in mind the various requirements for imaging, photometry and astrometry.

Imaging: In order to meet imaging sensitivity and contrast requirements the residual spectra of the atmosphere and ADC have to be kept below the 1 miliarcsecond level at all times. This is achieved by using the atmospheric parameters to correct the ADC rotation real time using a feed forward correction. Any offsets due to the changes in the absolute atmospheric refraction are automatically compensated by using a guide star for tracking the telescope.
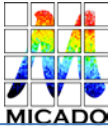
Photometry: The ADC temperature and rotation are monitored and stored in the FITS file. When stacking multiple images for Photometry, the ADC status information is used in an offline distortion model, reaching the 1 mili-arcsecond accuracy level for a images in order to allow accurate stacking of images. An alternative is to align sources individually before stacking using sub-image processing.

Astrometry: For optimal astrometry first the star type of each object must be determined using photometry data observed with at least 2 filters. Although this could also be obtained with a different instrument, MICADO itself is most ideally suited for this since it will provide images with the correct depth, spatial resolution and field of view. The atmospheric parameters are also stored in the FITS file. The atmospheric data, the ADC data and the star type are used together in an offline physical model of the entire system to generate detailed distortion corrections for each star in each exposure. The correction shall be accurate to the level of several micro arcseconds.

5.1 Possible Astrometry approach and operation scheme:

1. Measure atmosphere pressure, humidity, temperature
2. Model atmosphere dispersion
3. Measure ADC performance (model / inline measure rotation offsets + temperatures etc. / inline measure performance)
4. Exposures:
   a. Expose using filter 1
   b. Expose using filter 2
   c. Expose using filter 1
   d. Expose using filter 2
   e. etc.
5. From Photometric data: for each star model star type (color / magnitude)
6. For each star model atmosphere + ADC offset (per detector zone?)
7. For each star: fit to PSF and its pixilation for optimal astrometric position determination

5.2 Delivered data product for every star:

- Type (color / magnitude)
- Astrometric position

5.3 Instrument requirements:

- Time needed to switch between 2 filters < ~2 seconds (during readout of detector to minimize overhead)
- ADC requirements: performance per band ~1 mArcsec (normal ADC of 2 bi-material rotating prisms). This ADC should be located in a pupil plane to reduce astrometric errors and simplify manufacturing as no curved surfaces are required.
- A calibration mask should be provided before the ADC in order to calibrate the astrometric errors caused by the ADC.
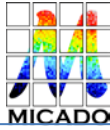
- Accurate measurement of temperature, pressure and humidity should be provided. Note that the Paranal astroclimatology page currently already provides temperature (~0.01°C), pressure (0.01 mbar) and humidity (1%). If similar data will be provided at E-ELT, at least temperature and pressure seem to be accurately available.

5.4 Draft Calibration Strategy

Calibration observations could be done using the calibration mask and astrometric reference fields.

5.5 Pipeline requirements

What can be concluded at this time is that the only way to achieve micro arcsecond astrometry is to do a real time correction of atmospheric effects using the ADC hardware, combined with post processing of the data using a physical model of the relevant parts and parameters of the instrument.

The residual atmospheric distortion and dispersion after ADC correction is linear to low-order as a function of zenith angle (especially if the source SEDs are known). Therefore it appears a worthwhile approach to fine-tune a physical model using the ensemble of observations over many nights. To make this type of calibration a more controlled experiment, one could explore the use of a polar astrometric reference field. Such a field would be observable every night of the year and therefore provide a long-term monitoring of the astrometric behavior of the instrument and accuracy of the physical model. In conclusion: long-term monitoring of astrometric reference field and calibrations using the calibration mask can validate the physical model approach and fine tune the model.

Due to the short duration of the study the implications for the astrometric pipeline are not fully assessed at this time. The requirement refers to the "best observational case". The atmospheric distortion with a best-case amplitude <~5mas center-to-edge needs to be modeled to the required ~10-50 micro-arcsecond accuracy. Constraints come from positional variations of extra-galactic sources (inter-epoch modeling) or all sources (intra-epoch) in the FoV. Further study is necessary to quantify this approach. Of special interest are the size and time scale for which distortions can be considered linear.

Also the accuracy of the prediction for the residual dispersion, considering the observed star type, needs to be further quantified. The ~3 micro-arcsecond effects in the best case are promising in terms of meeting the requirement.

Lastly, the changes in atmospheric conditions between observations (especially at different epochs) can cause ~50 micro-arcsecond distortions. A polar astrometric reference field would be very helpful to determine the accuracy of the physical model on this term.
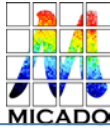
6   References

1. MICADO Compliance Matrix, E-TRE-MCD-561-0008
2. Call for Proposal For a Phase A Study of a High Angular Resolution Camera for the E-ELT, Specifications of the Instrument to be studied, E-ESO-SPE-561-0097, Issue 2.0
3. High-precision astrometry with MICADO at the European Extremely Large Telescope, Trippe et al., MNRAS 2010.
4. MICADO Phase A Scientific Analysis Report, E-TRE-MCS-561-0007, Issue 2.0, 19.10.2009
5. http://www.bo.astro.it/maory/Maory/Welcome.html
6. E-SPE-ESO-257-1270 Iss1 07.01.2013 - Top Level Requirements for ELT-CAM
7. Meyer 2011 - Astrometry with the MCAO instrument MAD
8. Neichel 2012 - Science Readiness of the Gemini MCAO System GeMS
9. Rigaut 2012 - GeMS First on-sky results
10. Fritz 2010 - What is limiting near-infrared astrometry in the Galactic Centre
11. Salas 2012 - The Infrared Imaging Spectrograph (IRIS) For TMT - Simulation of the Atmospheric Dispersion Corrector using IDL
12. Atad-Ettedgui 2008 - Atmospheric Dispersion Compensation for ELTs.
13. Goncharov 2007 - Atmospheric dispersion compensation for ELTs
14. Kopon 2010 - An Advanced Atmospheric Dispersion Corrector - The Magellan Visible AO Camera
15. Phillips 2010 - The Infrared Imaging Spectrograph (IRIS) for TMT the Atmospheric Dispersion Corrector
16. Pickles 1998 - A Stellar Spectral Flux Library: 1150-25000 Å